PCCP

Accepted Manuscript

ROYAL SOCIETY OF CHEMISTRY

www.rsc.org/pccp

TOC Summary and Graphic for Physical Chemistry Chemical Physics

Shih-Pin Chen and Ying-Chih Liao*

Phys. Chem. Chem. Phys. **2014**

Silver nanowires junctions are soldered chemically to form a stretchable conductor with great electrical conductivity in stretching or twisting process.

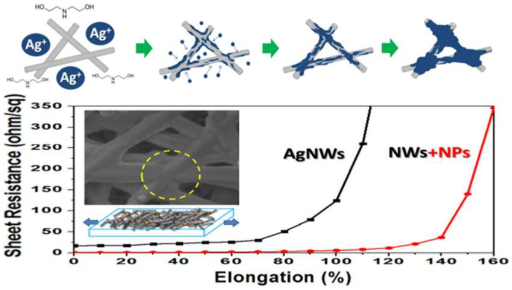

Journal Name RSCPublishing

COMMUNICATION

Cite this: DOI: 10.1039/x0xx00000x

Received 00th January 2012,
Accepted 00th January 2012

DOI: 10.1039/x0xx00000x

www.rsc.org/

Highly Stretchable and Conductive Silver Nanowire Thin Films by Soldering Nanomesh Junctions

*Shih-Pin Chen and Ying-Chih Liao**

Silver nanowires (AgNWs) have been widely used for stretchable and foldable conductors due to their percolating network nanostructure. To enhance the mechanical strength of AgNW thin films under extreme stretching conditions, in this study, we utilize a simple chemical reaction to join AgNW network connections. After applying a reactive ink over AgNW thin films, silver nanoparticles are preferentially generated over the nanowire junctions and solder the nanomesh structures. The soldered nanostructure reinforces the conducting network and exhibits no obvious change in electrical conductivity in stretching or rolling process with elongation strains up to 120%. Several examples are also demonstrated to show potential applications of this material on stretchable electronic devices.

Stretchable electronics has been perceived as a key technology for the realization of electronic applications in the next generation.[1] Unlike regular flexible electronics on paper or plastic sheets,[2, 3] the elastic nature of stretchable electronics enables a totally new design concept for electronic applications.[4] This new class of electronic devices can be bent, stretched, twisted, and deformed into complex, non-planar shapes while maintaining excellent performance, reliability, and integration. Recently, numerous attempts have been made to fabricate stretchable devices in a wide range of optoelectronic applications, such as solar cells,[5] polymer light-emitting devices (PLEDs),[6, 7] fuel cell,[8] and UV photodetectors (PDs).[9] In order to provide power to those devices, stretchable interconnects or wires with strong mechanical robustness and great electrical conductance are essential and of critical importance to the performance of these devices. However, in stretching or elastic deformation processes with large strains, it is difficult for traditional conductors, such as metal tracks or indium tin oxide (ITO) thin films, to maintain electrical conductivity simultaneously with mechanical stability. To overcome this problem, two main strategies have been used to manufacture stretchable conductors: (i) creating structural metal thin films,[10] and (ii) assembling nanomaterials on stretchable substrates. Typical examples using the first strategy include buckled serpentine metal structures on stretchable substrates[11] or metal thin films on pre-strained substrates[12] to preserve structural integrity of the laminated metal thin films at large strains. These conductors can maintain metallic conductivity in the stretching process. Alternatively, one can also directly deposit liquid solutions containing nano-structured materials, such as graphene,[13]

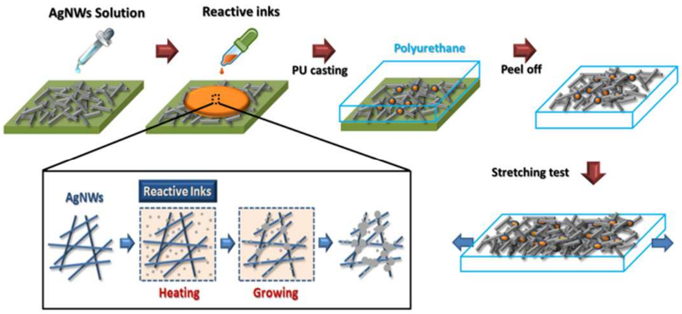

Figure 1. Schematic diagram of fabrication process for the highly stretchable and conductive metal conductors. Silver mirror reaction is triggered on AgNW networks to generate silver nanoparticles around AgNW junctions to reinforce both mechanical robustness and electrical conductivity. The composite Ag-NWs/NPs percolation networks are embedded within polyurethane to form stretchable conductive thin films.

carbon nanotube,[1] and metal nanowires (m-NWs),[12, 14-16] on elastic substrates with spin coating or electrospinning[17] methods to form stretchable conductors. Among these nano-materials, m-NWs have recently attracted wide attentions for their high mechanical flexibility, great electrical conductivity, and good optical transparency. As indicated by a series of recent research,[16] as one increases the length or aspect ratios of m-NWs, the percolating networks of m-NW thin films can more effectively accommodate strains and show good tolerance in stretching process. Moreover, their mesh-like geometries not only can serve as an outstanding electric charge transport medium but also allow light penetration as well. Therefore, stretchable conductors with m-NWs can maintain high conductivity as well as great transparency and are considered as promising electrode candidates for electronic devices in the next generation.

Stretchable metal nanowire thin film conductors are regularly manufactured by solution-based processes for the high fabrication speed at low cost. One of the challenges to implement m-NWs for thin film conductors is that the insulating ligands used in the synthesis or solution dispersion must be removed after film deposition to ensure effective electrical contacts between m-NWs. This step is regularly completed by post-treatments, such as thermal heating,[18] capillary-force-assisted stiction,[19] mechanical pressing[20] or plasmonic welding,[21-23] to reduce the contact resistance between nanowires. To enhance the conductivity of m-NW networks and to avoid resistance between NW junctions, Ko et al.[16, 24, 25] even synthesized very long m-NWs and showed great results in both conductivity and stretchability. Different from those methods in the literature, here we demonstrate a new chemical soldering method to enhance silver nanowire (AgNW) network connections with a simple and fast solution-based process. The fabrication process of silver NWs/NPs electrodes on stretchable polyurethane (PU) substrates is illustrated in Figure 1. AgNWs dispersion was first spin coated on a glass plate. After drying, a reactive ink is spread on the AgNW thin film. The reaction turns silver ions into silver nanoparticles, which preferentially grow on AgNW junctions, and chemically solder the AgNW network. Then, liquid PU solution was poured on top of the soldered AgNW thin film. The dried PU films were then peeled off from the glass plate and the electrical conductivities of AgNW thin films on PU were measured. The chemically soldered AgNW networks show great enhancement in in electrical conductivity and exhibit no obvious change even at large tensile strain (>120%).

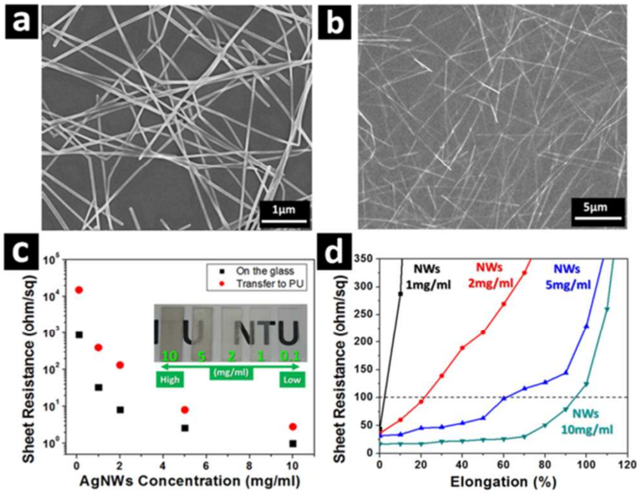

Figure 2. (a) SEM image of the pristine AgNW film on a glass plate. (b) SEM image of the AgNW film after transferred to polyurethane (PU) substrates. (c) Variation of sheet resistance with AgNW concentrations before and after transferred to polyurethane (PU) substrate. The inset in (c) shows the images of pure AgNW thin films spin-coated at different concentrations on PU substrates. (d) Variation of electrical resistances with elongation strains for AgNW thin films on PU substrates. The samples were prepared with different AgNW concentrations as indicated in the figure.

At first, we examine carefully the microstructures and electrical performance of pure AgNW thin films cast in PU substrates. Figure 2a shows the top-view SEM image of AgNWs structure after coated on glass. The AgNWs spread uniformly with numerous crossover junctions, which provide efficient electron transfer routes for electrical conduction. When the liquid PU was poured onto the cast AgNW film, the liquid not only filled into the space between nanowires (Figure 2b) but might also seep into the junction gaps between nanowires. Consequently, the junction contacts between nanowires can be less efficient for electron transfer after the cast-peeling process. Thus, larger sheet resistances were observed after AgNWs transferred to PU (Figure 2c). The sheet resistance and optical transparency of the nanowire coating on glass depend also strongly on the applied AgNWs concentration. Higher AgNW density leads to lower electrical resistance, but also results in higher transparency loss (inset picture in Figure 2c). The sheet resistances of AgNW thin films before and after the cast-peeling process, however, are roughly of the same order, indicating that the cast-peeling process causes no extreme changes in AgNW networks. Next, the variation in electrical resistance in the stretching process for films with different AgNW amounts is compared (Figure 2d). For films made of low AgNW concentration (1 mg/ml), the electrical resistance increases rapidly with tensile strain, and the conductor even becomes non-conductive at ~15% elongation strain because of network failure or localized fractures.[26, 27] As the concentration of AgNW increases, more junctions between nanowires exist and thus can maintain AgNW network connections at larger elongations. As

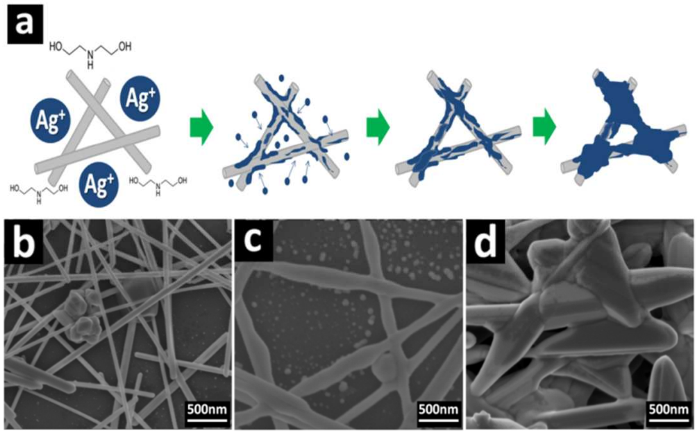

Figure 3 (a) Schematic diagram of the nano-soldering process. SEM images of AgNW structures after applying the silver ink for (b) 1 min, (c) 5 min, and (d) 10 min.

shown in Figure 2d, if spin-coated with 10 mg/ml AgNW solution, the conductive AgNW films cast on PU can have low resistance (~120 Ω) even at 100% strain. These data indicate that the connections between AgNW networks are of critical importance for efficient electron transfer at stretching conditions. Thus, if one can buttress the connections between wires, the electrical conductivity under stretching conditions can be greatly enhanced.

To enhance the conductivity of stretchable AgNW films, the wire/wire junctions are chemically soldered with a reactive silver ink. After applying the silver ink over AgNW network, silver nanoparticles were recovered over the AgNWs, and gradually wrapped over the AgNW surfaces (Figure 3a). The silver recovery process of the applied ink is a two-step reaction involving the self-degradation of diethanolamine (DEA) and silver mirror reaction.[28] The formaldehyde accompanying with DEA degradation works as a reduction agent and recovers silver ions (Ag^+) quickly to form silver nanoparticles.[23] As the silver mirror reaction proceeds, because the existing metal surface provides better electron exchange sites for the redox reaction, the recovered silver prefer to crystalize along the AgNW surfaces. Moreover, because there are more accessible metal surface areas around the AgNW junctions, silver ions have much higher tendency to be reduced near the junctions. As depicted in Figure 3b-d, because of the enlargement of AgNW diameter (Figure S2) by reduced silver, the junction gaps between AgNWs were filled and fused the junctions. As reaction proceeds, the filled junctions kept on growing and became larger than the wires. Finally, the generated silver crystals covered the whole empty areas between nanowires after 10 minutes.

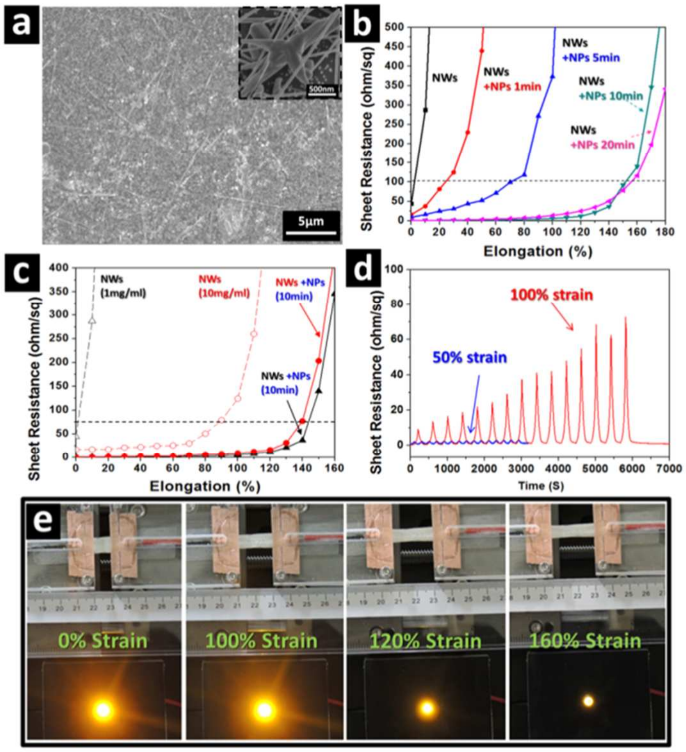

Figure 4. (a) SEM image of chemically soldered AgNW film embedded in polyurethane. The inset is an enlarged image of a chemically soldered AgNW junction. (b) Evolution of film resistances of pristine AgNW thin film (prepared with 1 mg/ml AgNW solution), and the chemically soldered AgNW networks with different reaction times. The films are all embedded in PU substrates and have a dimension of 1 cm × 1 cm. (c) Comparison of electric resistances of soldered AgNW thin films with different AgNW concentrations. (d) Resistance responses of stretching films under elongation cycles of triangular waveforms at various strain rates. The pulsating strain rate is 0.005 s^{-1}. (e) Images of LED light connected with a stretchable conductor at various strain conditions. The sample conductor was prepared with 1 mg/ml AgNW solution with chemical soldering for 10 minutes.

The chemically soldered AgNW thin films can be transferred on PU (Figure 4a), and show not only higher electrical conductivity but also better mechanical endurance during stretching process. As shown in Figure 4b, the AgNW thin film, which originally is non-conductive at 10% strain, turns out to be elastically conductive even under 20-40% strain after chemically soldered for merely 1 minute, indicating that the reinforcement of AgNW network junctions leads to conductivity enhancement at higher strain conditions. With longer reaction time, more silver was recovered on AgNW surfaces and the AgNW networks become more tightly connected. The wire/wire contacts became larger and stronger, leading to lower resistance at higher elongation. The soldered AgNW thin films have a much lower resistance at rest, and remain conductive even at large elongation of 160% elongation. However, the enhancement of elastic conductivity with chemical soldering process reached a limit after 10 minute soldering time. For reactions longer than 10 minutes, the recovered silver might occupy nearly all the space between the nanowires, and thus the soldering effect between AgNW junctions reaches its maximum. Therefore, the stretching resistance curves for those thin films soldered with 10 and 20 minutes virtually overlap. The chemically soldered AgNW films remain partly transparent. The transmittance reduces with longer sintering time, and ranges from 30-80% for visible lights (Figure S1(b)). Thus, one can also prepare transparent films with great elastic conductivity with this chemical soldering method by carefully adjusting the soldering time.

Another feature of this chemical soldered conductor is that only little amount of AgNW is needed for high electrical conductivity at high strain conditions. For pure AgNW thin films, the major electron transfer resistance comes from the partial contact between nanowires. Thus, the resistance can be greatly reduced with more AgNW coverage on the substrate surface simply as a result of more AgNW contacts. As the film stretches, the elongation can lead to dislocation of the contact points, leading to higher electrical resistance. On the other hand, for soldered AgNW thin films, because the nanowire joints has been cemented by silver nanoparticles, the AgNW network remains intact under stretching conditions. Thus, as long as there are percolating filaments of AgNW on the surface, the soldered network can provide great paths for electron transfer with strong mechanical stability regardless of AgNW amount. As shown in Figure 4c, the resistance-strain curves of soldered thin films made from 1 mg/ml and 10 mg/ml AgNW solutions almost overlap, indicating that the film conductivity is independent of the applied amount of AgNWs after chemical soldering.

The soldered nanomesh structures also make the composite AgNW/AgNP thin films fairly robust to fast elastic deformation.

Figure 4d shows the electrical responses of the AgNW/AgNP films under elongation cycles with a triangular waveform (Figure S3(a)). At moderate strains, say 50% deformation, the films remain highly conductive with little resistance variation (~2Ω). With a large strain amplitude (100%), the deformation leads to certain structural damages on AgNW network integrity and thus the peak resistance increases with the number of pulsating cycles. At faster strain rates (0.05 s^{-1}, see Figure S3(b)), the resistance variation during the triangular pulsation is roughly the same for moderate strain (50%) as those of slow strain rate. However, the deformational damages with 100% strain were more pronounced, and the peak resistance rises faster than that at slower strain rate of 0.005s^{-1}. Nevertheless, as the deformation pulsation stops, the resistance of the films returns to the original value, indicating that the films are fairly durable during the stretching pulsations.

The great conductivity at large strain condition makes the chemically soldered thin films an ideal elastic conductor material for electronic applications. Figure 4e demonstrates such an example. A soldered thin film conductor is connected in series with a LED and a power supply at a constant voltage. As the conductor being stretched, nearly no brightness change in the LED light is observed for strains below 100%, and the LED still remains bright even when the conductor is stretched at 160%. This example indicates that the conductor made by this soldering process can be easily applied in electrical devices to serve as elastic conductive tracks. Besides regular stretching applications, the great strain endurance and high conductivity of the chemically soldered AgNW films can also be utilized to fabricate various devices under extreme deformation conditions, such as twisting (Figure S4), bending, and elongation (Figure S5). Those applications show that the soldered AgNW thin films not only can endure large strain in elongation process but also remain conductive under strains from multiple directions. One can also make AgNW thin film patterns (Figure S6) with this chemical soldering method for stretchable interconnects or RFIDs.

Conclusions

In summary, this work presents a new fabrication method for highly stretchable and conductive metal electrodes with the aid of a newly developed synthesis method at low temperatures. After applying the reactive inks on a spin-coated AgNW thin film, silver mirror reaction occurs preferentially on the surfaces of AgNWs, and chemically solders the AgNWs to form a mechanically stronger network. The reinforced AgNW mesh frameworks can accommodate significant longitudinal strains at extreme stretching conditions, and possess much lower electrical resistance and stronger robustness against electrical disconnections or breakdown in stretching process. With this chemical solder process, films with considerably little AgNW amount can exhibit great electrical performance in the stretching process. Thus, this synthetic route not only enables the fabrication of highly stretchable conductive films, but also helps to reduce the usage of AgNW. We also demonstrate the feasibility of applying the synthesized AgNW/AgNP stretchable conductors for mobile touching LED circuits. We believe that this chemical soldering method can effectively solve the interconnection problems for elastic conductors and provides a promising strategy toward flexible, wearable, and stretchable electronic devices for the next generation electronics.

Acknowledgement

National Science Council in Taiwan supported this research through Grants MOST 103-2923-E-002-010-MY3 and NSC 101-2221-E-002-177-MY2.

Notes and references

[a] No. 1, Sec. 4, Roosevelt Road, Taipei, 10617 Taiwan. Department of Chemical Engineering, National Taiwan University, Taiwan; E-mail: liaoy@ntu.edu.tw

† Electronic Supplementary Information (ESI) available: experimental details, transmittance data, and exemplar applications. See DOI: 10.1039/c000000x/

1 Rogers, J. A.; Someya, T.; Huang, Y. *Science* 2010, **327**, 1603.
2 Mazzeo, A. D.; Kalb, W. B.; Chan, L.; Killian, M. G.; Bloch, J. F.; Mazzeo, B. A.; Whitesides, G. M. *Adv. Mater.* 2012, **24**, 2850.
3 Yang, C.; Gu, H.; Lin, W.; Yuen, M. M.; Wong, C. P.; Xiong, M.; Gao, B. *Adv. Mater.* 2011, **23**, 3052.
4 Sekitani, T.; Someya, T. *Adv. Mater.* 2010, **22**, 2228.
5 Lipomi, D. J.; Tee, B. C.; Vosgueritchian, M.; Bao, Z. *Adv. Mater.* 2011, **23**, 1771.
6 Liang, J.; Li, L.; Niu, X.; Yu, Z.; Pei, Q. *Nat. Photonics* 2013, **7**, 817.
7 White, M. S.; Kaltenbrunner, M.; Glowacki, E. D.; Gutnichenko, K.; Kettlgruber, G.; Graz, I.; Aazou, S.; Ulbricht, C.; Egbe, D. A. M.; Miron, M. C.; Major, Z.; Scharber, M. C.; Sekitani, T.; Someya, T.; Bauer, S.; Sariciftci, N. S. *Nat. Photonics* 2013, **7**, 811.
8 Chang, I.; Park, T.; Lee, J.; Lee, H. B.; Ji, S.; Lee, M. H.; Ko, S. H.; Cha, S. W. *Int J Hydrogen Energ* 2014, **39**, 7422.
9 Yan, C. Y.; Wang, J. X.; Wang, X.; Kang, W. B.; Cui, M. Q.; Foo, C. Y.; Lee, P. S. *Adv Mater* 2014, **26**, 943.
10 Guo, C. F.; Sun, T.; Liu, Q.; Suo, Z.; Ren, Z. *Nat. Commun.* 2014, **5**, 3121.
11 Kim, D.-H.; Xiao, J.; Song, J.; Huang, Y.; Rogers, J. A. *Adv. Mater.* 2010, **22**, 2108.
12 Wang, X.; Hu, H.; Shen, Y.; Zhou, X.; Zheng, Z. *Adv. Mater.* 2011, **23**, 3090.
13 Lee, M. S.; Lee, K.; Kim, S. Y.; Lee, H.; Park, J.; Choi, K. H.; Kim, H. K.; Kim, D. G.; Lee, D. Y.; Nam, S.; Park, J. U. *Nano Lett.* 2013, **13**, 2814.
14 Xu, F.; Zhu, Y. *Adv. Mater.* 2012, **24**, 5117.
15 Yun, S.; Niu, X.; Yu, Z.; Hu, W.; Brochu, P.; Pei, Q. *Adv. Mater.* 2012, **24**, 1321.
16 Lee, P.; Lee, J.; Lee, H.; Yeo, J.; Hong, S.; Nam, K. H.; Lee, D.; Lee, S. S.; Ko, S. H. *Adv. Mater.* 2012, **24**, 3326.
17 Wu, H.; Kong, D. S.; Ruan, Z. C.; Hsu, P. C.; Wang, S.; Yu, Z. F.; Carney, T. J.; Hu, L. B.; Fan, S. H.; Cui, Y. *Nat. Nanotechnol.* 2013, **8**, 421.
18 Madaria, A.; Kumar, A.; Ishikawa, F.; Zhou, C. *Nano Res.* 2010, **3**, 564.
19 Lee, J.; Lee, P.; Lee, H. B.; Hong, S.; Lee, I.; Yeo, J.; Lee, S. S.; Kim, T. S.; Lee, D.; Ko, S. H. *Adv. Funct. Mater.* 2013, **23**, 4171.
20 Tokuno, T.; Nogi, M.; Karakawa, M.; Jiu, J.; Nge, T. T.; Aso, Y.; Suganuma, K. *Nano Res.* 2011, **4**, 1215.
21 Garnett, E. C.; Cai, W. S.; Cha, J. J.; Mahmood, F.; Connor, S. T.; Christoforo, M. G.; Cui, Y.; McGehee, M. D.; Brongersma, M. L. *Nat. Mater.* 2012, **11**, 241.
22 Zhu, S.; Gao, Y.; Hu, B.; Li, J.; Su, J.; Fan, Z.; Zhou, J. *Nanotechnology* 2013, **24**, 335202.

23 Han, S.; Hong, S.; Ham, J.; Yeo, J.; Lee, J.; Kang, B.; Lee, P.; Kwon, J.; Lee, S. S.; Yang, M. Y.; Ko, S. H. *Adv. Mater.* 2014.
24 Lee, J.; Lee, P.; Lee, H.; Lee, D.; Lee, S. S.; Ko, S. H. *Nanoscale* 2012, **4**, 6408.
25 Lee, J. H.; Lee, P.; Lee, D.; Lee, S. S.; Ko, S. H. *Cryst. Growth Des.* 2012, **12**, 5598.
26 Hu, W.; Niu, X.; Li, L.; Yun, S.; Yu, Z.; Pei, Q. *Nanotechnology* 2012, **23**, 344002.
27 Lee, I.; Lee, J.; Ko, S. H.; Kim, T. S. *Nanotechnology* 2013, **24**.
28 Chen, S. P.; Kao, Z. K.; Lin, J. L.; Liao, Y. C. *ACS Appl. Mater. Interfaces* 2012, **4**, 7064.